Allergologia et immunopathologia
Sociedad Española de Inmunología Clínica, Alergología y Asma Pediátrica
www.all-imm.com

RESEARCH ARTICLE OPEN ACCESS

Triamcinolone acetonide induces the autophagy of Ag85B-treated WI-38 cells via SIRT1/FOXO3 pathway

Li Luo[a,#], Lei Zhou[a,#], Linzi Luo[a], Dan Feng[a], Yan Ding[a], Zhibin Lu[a], Ganjuan Nie[b], Liqiong Bai[c], Yangbao Xiao[a*]

[a]*Endoscopy Center, Hunan Chest Hospital, Changsha, Hunan, China*
[b]*Department of Pathology, Hunan Chest Hospital, Changsha, Hunan, China*
[c]*Hunan Chest Hospital, Changsha, Hunan, China*

[#]*Li Luo and Lei Zhou contributed equally to this work and share first authorship.*

Received 14 September 2022; Accepted 17 October 2022
Available online 1 March 2023

KEYWORDS
autophagy;
SIRT1/FOXO3 pathway;
tracheobronchial stenosis due to tuberculosis;
triamcinolone acetonide

Abstract
Background: Tracheobronchial stenosis due to tuberculosis (TSTB) seriously threatens the health of tuberculosis patients. The inflammation and autophagy of fibroblasts affect the development of TSTB. Triamcinolone acetonide (TA) can regulate the autophagy of fibroblasts. Nevertheless, the impact of TA on TSTB and underlying mechanism has remained unclear.
Objective: To study the impact of TA on TSTB and underlying mechanism.
Material and Methods: In order to simulate the TSTB-like model *in vitro*, WI-38 cells were exposed to Ag85B protein. In addition, the *cell counting kit* (CCK)-8 assay was applied to assess the function of TA in Ag85B-treated WI-38 cells. Quantitative real-time polymerase chain reaction was applied to detect the mRNA level of sirtuin 1 (SIRT1) and forkhead box O3 (FOXO3a), and autophagy-related proteins were evaluated by Western blot analysis. Vascular endothelial growth factor (VEGF) level was investigated by immunohistochemical staining. Enzyme-linked immunosorbent serologic assay was applied to detect the secretion of inflammatory cytokines. Furthermore, hematoxylin and eosin staining was applied to observe tissue injuries.
Results: Ag85B affected WI-38 cell viability in a limited manner, while TA notably suppressed Ag85B-treated WI-38 cell viability. TA induced the apoptosis of Ag85B-treated WI-38 cells in a dose-dependent manner. In addition, Ag85B-treated WI-38 cells demonstrated the upregulation of interleukin (IL)-6, tumor necrosis factor-α (TNF-α), i*nterferon gamma* (IFN-γ), and fibrotic proteins (transforming growth factor-beta [TGF-β] and vascular endothelial growth factor [VEGF]), which can be significantly destroyed by the TA. Meanwhile, TA reversed Ag85-induced inhibition of cell autophagy by mediation of p62, LC3, and Beclin1. Furthermore, silencing of SIRT1/FOXO3a pathway could reverse the effect of TA on the autophagy of Ag85B-treated cells.

***Corresponding author:** Yangbao Xiao, Hunan Chest Hospital, No. 519, Xianjiahu Road, Yuelu District, Changsha City, Hunan Province, China. *Email address*: xybsnow@163.com

https://doi.org/10.15586/aei.v51i2.775

Conclusion: TA significantly induced the autophagy of fibroblasts in Ag85B-treated cells by mediation of SIRT1/FOXO3 pathway. This study established a new theoretical basis for exploring strategies against TSTB.

Introduction

Tracheobronchial stenosis due to tuberculosis (TSTB) is one of the frequent complications of tuberculosis (TB). It was estimated that about 90% of patients with tracheobronchial TB could have some degree of tracheal or bronchial stenosis.[1,2] The components of mycobacterium TB, immune response against mycobacterium TB, and genetic factors cause excessive proliferation of fibroblasts, granulation tissue hyperplasia, increased collagen fiber synthesis, cell proliferation, and extracellular matrix (ECM) deposition, which results in narrowing of the airway.[3,4] Meanwhile, multiple inflammatory cytokines are involved in the defense mechanism against mycobacterium TB infection,[5] and inflammatory cytokines could promote the proliferation of fibroblasts, which further narrows down the airway.[6] At present, only few studies have discussed TSTB.

Autophagy is a subtype of cellular process through which proteins caused by cellular stress decline.[7] Autophagy has played a protective role in a rabbit model of tracheal stenosis, and activation of autophagy could be an effective therapy.[8] Rapamycin-induced enhancement of autophagy improved Bacillus of Calmette and Guérin (BCG) delivery to lysosomes, improved antigen expression on CD4 and CD8 T cells, and significantly enhanced anti-TB efficacy in mice.[9,10] In liver fibrosis models, corresponding drugs can increase the clearance of ECM deposition by upregulating Beclin1 (core protein in autophagy)-induced autophagy.[11] Hence, autophagy could play a protective role in fibrosis. However, the detailed effect of autophagy in TSTB progression remains unclear.

Triamcinolone acetonide (TA) is a synthetic corticosteroid with anti-inflammatory properties.[12] It is often used clinically to prevent fibrosis-related dysfunction.[13] Chen et al. suggested that intra-injection of TA significantly induced keloid cell apoptosis and inhibited keloid formation.[14] In addition, TA combined with 5-fluorouracil inhibited autophagy and fibrosis in urethral scar fibroblasts by increasing the expression of miR-192-5p.[15] Nevertheless, the effects of TA in TSTB are not clear.

Therefore, this study explored the effect and potential mechanism of TA on TSTB, and provided a new theoretical basis for exploring strategies against TSTB.

Materials and Methods

Clinical sample collection

The adjacent normal tissue samples of nonsmoker patients with lung cancer, as well as the bronchial tissue samples of patients with tuberculous proliferative airway stenosis (TPTS) or tuberculous cicatricial airway stenosis (TSTS), were obtained from Hunan Chest Hospital between August 2020 and September 2021. Clinical and pathological data of these patients were collected after having their written informed consent. This research was approved by the Institutional Ethical Committee of Hunan Chest Hospital. The tissues were stored at −80°C.

Cell culture and treatment

Human embryonic lung fibroblasts (WI-38 and CL-0243; Pricella, China) were cultured in Dulbecco's modified eagle *medium (*DMEM, 11965092; Thermo Fisher Scientific, MA, USA) containing 10% fetal bovine serum (FBS, 04-001-1ACS; Gibco, USA) and 1% streptomycin–penicillin (15140122; Thermo Fisher) at 37°C and 5% CO_2. WI-38 cells were exposed to 0.5-, 1-, 2-, 4-, or 8-μg/mL recombinant mycobacterium TB major secretory protein antigen 85B (Ag85B, ab83471; Abcam, Cambridge, UK) to simulate a TSTB-like model *in vitro*. In addition, to assess the function of TA in the TSTB-like model, cells were exposed to 0-, 5-, 10-, or 20-μM TA (T6376; Sigma, USA) for 24 h. Meanwhile, to investigate the role of autophagy in TA-mediated TSTB progression, cells were treated with 3-methyladenine (3-MA) autophagy inhibitor (189490; Sigma).

Cell transfection

WI-38 cells (3×10^5 cells/well) were cultured. When cells reached 70% confluence, they were transfected with Sirtuin 1 (SIRT1) small interfering RNA (siRNA) or negative control (NC, GenePharma, Shanghai, China) for 48 h using lipofectamine 2000 (Invitrogen, MA, USA) according to manufacturer's protocol to silence SIRT1 (si-SIRT1).

To overexpress SIRT1 (oe-SIRT1), glioma cells were exposed to plasmid cloning (pc)DNA3.1 vector or pcDNA3.1-SIRT1 using lipofectamine 2000. Both pcDNA3.1-SIRT1 and pcDNA3.1 were obtained from GenePharma.

Cell counting kit (CCK-8) assay

WI-38 cells (5×10^3 per well) were seeded overnight. Thereafter, cells were exposed to different concentrations of TA for 24 h. CCK-8 10% (NU679; Dojindo Laboratories, Japan) was added to the cells at 37°C for 2 h. Finally, a microplate reader (MB-530; Huisong, China) was used to assess optical density ($OD_{450\ nm}$).

Western blot analysis

Radioimmunoprecipitation assay (RIPA; Beyotime Biotechnology, Shanghai, China) buffer was applied to

extract total protein. Bicinchoninic acid (BCA) assay kit (Beyotime) was applied for protein quantification. Sodium dodecyl sulfate–polyacrylamide gel electrophoresis (SDS-PAGE 10%) was applied to separate proteins (40 μg per lane). Subsequently, proteins were collected on polyvinylidene fluoride (PVDF) membranes (Invitrogen). After 5% skimmed milk was applied to block membranes for 1 h, the following primary antibodies were applied to incubate membranes overnight: anti-SIRT1 (13161-1-AP, 1:3000; ProteinTech, IL, USA), anti-forkhead box O3 (FOXO3a) (10849-1-AP, 1:1000; ProteinTech), anti-p65 (10745-1-AP, 1:2000; ProteinTech), anti-acetylated p65 (ac-p65, #12629, 1:1000; CST, USA), anti-transforming growth factor-beta1 (TGF-β1) (ab31013, 1:1000, Abcam), anti-VEGF (19003-1-AP, 1:1000; ProteinTech), anti-LC3 (18725-1-AP, 1:500; ProteinTech), anti-Beclin1 (11306-1-AP, 1:5000; ProteinTech), anti-p62 (18420-1-AP, 1:5000; ProteinTech), and anti-β-actin (66009-1-Ig, 1:5000; ProteinTech). Thereafter, secondary antibodies (HRP-conjugated, 1:5000; Abcam) were applied to incubate the membranes for 1 h. Enhanced chemiluminescence (ECL) kit (Thermo Fisher) was applied to analyze protein bands, and β-actin was applied for data quantification.

Co-Immunoprecipitation (Co-IP)

Cells were lysed with pre-cooled RIPA lysis buffer, and a 15-min centrifugation (at 14,000 × g, 4°C) was performed and the supernatant was transferred in a new tube. Anti-FOXO3a (10849-1-AP, 1:1000; ProteinTech) was added to 200-μL cell lysate, and immunoglobulin G (IgG) antibody (B900610; ProteinTech) was added to negative control group. The antigen–antibody mixture was slowly shaken overnight at 4°C or for 2 h at room temperature using a shaker. After that, the mixture was added to 20-μL protein A/G agarose beads (prepared in phosphate-buffered saline [PBS] solution with a concentration of 50%) and mixed at 4°C overnight or incubated for 1 h. The agarose beads–antigen–antibody complex was harvested after a 5-s centrifugation and supernatant removal. Next, the complex was rinsed with pre-cooled RIPA buffer (800 μL) and suspended with 2× loading buffer (60 μL). The sample was boiled for 5 min and centrifuged to collect remaining agarose beads, and the supernatant was boiled again for 5 min and electrophoresed. Western blot analysis was used to test ac-FOXO3a (ab190479, 1:2000; Abcam) expression.

Immunofluorescence

Paraform (4%) was applied to prefix cells for 30 min. Subsequently, pre-cold methanol was applied to fix the cells for 10 min. Primary antibodies were applied to incubate the cells at 4°C overnight: anti-LC3 (ab192890, 1:150; Abcam), anti-SIRT1 (13161-1-AP, 1:50; ProteinTech), and anti-Beclin1 (14132-1-AP, 1:50; ProteinTech). Goat anti-rabbit IgG antibody (SA00013-2, 1:100; ProteinTech) was regarded as the secondary antibody. 4′,6-Diamidino-2-phenylindole (DAPI) was applied to stain nuclei for 15 min. Fluorescence microscope (Olympus CX23; Olympus, Japan) was used to observe the sample.

Enzyme-linked immunosorbent serologic assay (ELISA)

Levels of tumor necrosis factor-α (TNF-α, CSB-E04740h), interleukin (IL)-6 (CSB-E04638h), and *interferon gamma* (IFN-γ, CSB-E04577h) in WI-38 cells supernatant were evaluated by ELISA kit (CUSABIO, Wuhan, China).

Quantitative real-time polymerase chain reaction (RT-qPCR)

TRIzol (TaKaRa, Japan) was applied to extract total RNA in line with the manufacturer's protocol. PrimeScript kit (TaKaRa) was applied to synthesize complementary DNA (cDNA) in accordance with the manufacturer's protocol. ABI7500 system was applied in RT-qPCR analysis using SYBR Green. RT-qPCR was done in the following manner: 94°C for 2 min, followed by 35 cycles (at 94°C for 30 s and at 55°C for 45 s). The primers were obtained from GenePharma. $2^{-\Delta\Delta CT}$ was applied for data quantification, and β-actin was used for normalization. The following primers were applied: SIRT1: forward, 5'-ATTCCAAGTTCCATACCCCAT-3′ and reverse 5'-TGGCATATTCACCACCTAACCT-3′; FOXO3a: forward, 5'-GACTTTGCCTCTACCTAGTGAACCC-3′ and reverse 5'-TTTATTTCCCCTCGCAAGTCCT-3′; and β-actin: forward, 5'-ACCCTGAAGTACCCCATCGAG-3′ and reverse 5'-AGCACAGCCTGGATAGCAAC-3′.

Cell apoptosis analysis

Cells were trypsinized, washed, and resuspended in Annexin V buffer. Subsequently, APC (5 μL) and propidium (PI, 5 μL) were applied to stain cells with no light for 15 min according to the apoptosis kit (KGA1030-1007; KeyGEN BioTECH, China). Flow cytometery (BD; Franklin Lake, NJ, USA) was applied to analyze apoptotic cells.

Immunocytochemistry (ICC)

Paraformaldehyde (4%) was applied to fix cells overnight. Subsequently, paraffin-embedded cells were cut into 5-μm-thick sections. After rehydration, sections were heated in a microwave for antigen retrieval, and PBS was applied to wash sections for 5 min. After that, H_2O_2 (3%) was used to incubate samples for 25 min. Then, goat serum was employed to incubate samples for 30 min after these were washed with PBS. Primary antibodies (anti-VEGF, ab2349; Abcam) were used to stain samples at 4°C overnight, and secondary antibody (HRP-labeled) was applied to incubate the same for 30 min. Finally, 3,3′-diaminobenzidine (DAB) was used for color development. All the antibodies were obtained from Abcam. A fluorescence microscope was used to study positive cells.

Hematoxylin and Eosin (H&E) staining

Paraformaldehyde (4%) was applied to fix tissues for 24 h; then these were paraffin-embedded and sectioned (4 μm). Next, gradient alcohol was used to dehydrate sections,

and the same were cleared and mounted. H&E solution (Beyotime) was applied to stain mounted sections. Finally, tissue injury was evaluated under a light microscope.

Statistical analysis

Three independent experiments were applied in each group, and mean ± standard deviation (SD) was applied to express the data. One-way analysis of variance (ANOVA) followed by Tukey's test (more than two groups) or Student's *t*-test (only two groups) was applied via Graphpad Prism7 to analyze changes; $P < 0.05$ was considered as statistically significant.

Results

SIRT1 was downregulated in TSTB

H&E staining was performed to assess the role of SIRT1 in TSTB. As revealed in Figure 1A, significant fibroblasts and inflammatory infiltration were observed in TPTS and TSTS, and the data of immunofluorescence staining confirmed that SIRT1 was decreased in TSTB (Figure 1B). The expressions of SIRT1 and FOXO3a were significantly lower in the TPTS and TSTS, compared to those in the normal group. In contrast, the levels of ac-FOXO3a, TGF-β1, and VEGF were much higher in TPTS and TSTS than those in the normal group (Figures 1C and D). Meanwhile, Western blot analysis was used to detect the role of autophagy in TSTB. In both TPTS and TSTS tissues, the LC3B and Beclin1 expressions were lower than that in the normal group, while the level of p62 exerted opposite trend (Figure 1E). Consistently, the development of TSTB significantly promoted the secretion of pro-inflammatory cytokines (TNF-α, IL-6, and IFN-γ; Figure 1F).

Triamcinolone acetonide-induced apoptosis in Ag85B-treated cells

To mimic a TSTB-like model *in vitro*, WI-38 cells were exposed to Ag85B. In Figure 2A, Ag85B limitedly affected the viability of cells. In addition, the levels of TGF-β1 and VEGF in WI-38 cells were upregulated by Ag85B (Figure 2B), and Ag85B could notably upregulate TNF-α, IL-6, and IFN-γ levels in WI-38 cell supernatants (Figure 2C). Since Ag85B (2 μg/mL) exerted the most remarkable effect on fibrosis and inflammation, it was selected for use in subsequent analysis. Then, the viability of Ag85B-treated WI-38 cells was inhibited by TA (Figure 2D). Furthermore, TA induced apoptosis in Ag85B-treated WI-38 cells in a dose-dependent manner (Figure 2E). Based on the above results, TA (20 μM) was selected in our study. Taken together, TA significantly induced apoptosis in Ag85-treated WI-38 cells.

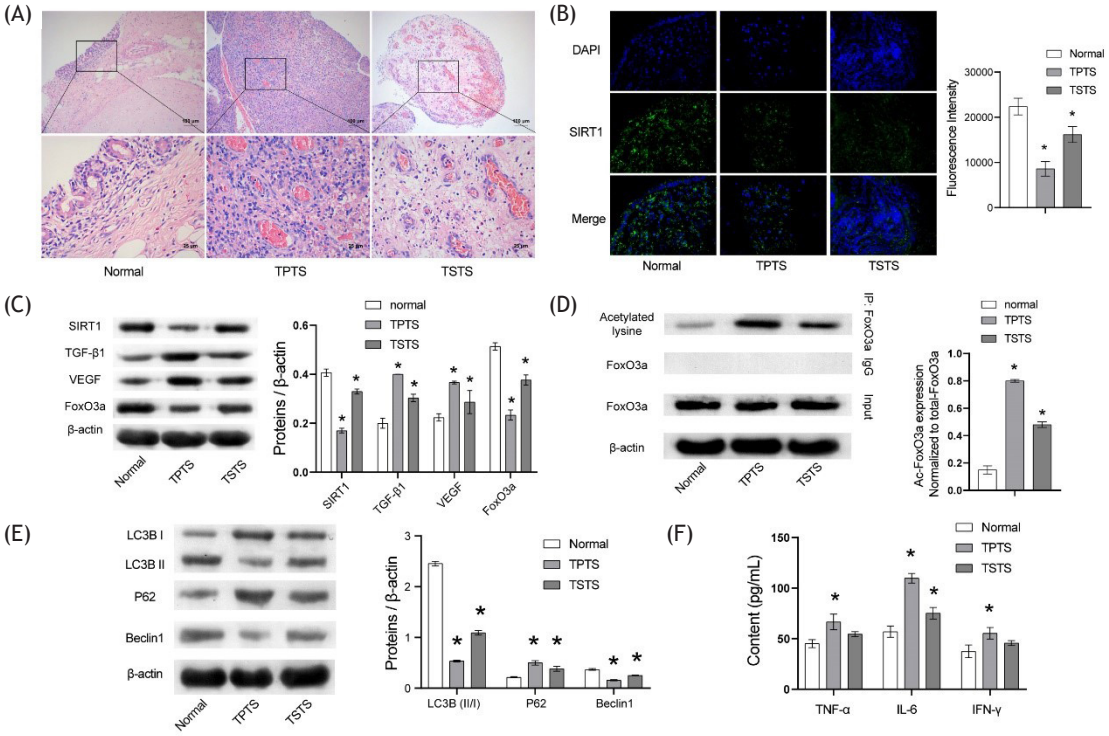

Figure 1 The SIRT1 and FOXO3a levels were downregulated in TSTS and TSTS. (A) The tissue injury was observed by H&E staining. (B) The expression of SIRT1 in tissues was detected by immunofluorescence staining. (C and D) The protein levels of SIRT1, TGF-β1, VEGF, FOXO3a, and ac-FOXO3a were detected by Western blot analysis. (E) The protein levels of LC3 II/I, Beclin1, and p62 in tissues were investigated by Western blot analysis. (F) The concentrations of IL-6, TNF-α, IFN-γ in the serum of patients were assessed by ELISA. *$P < 0.05$, compared to normal.

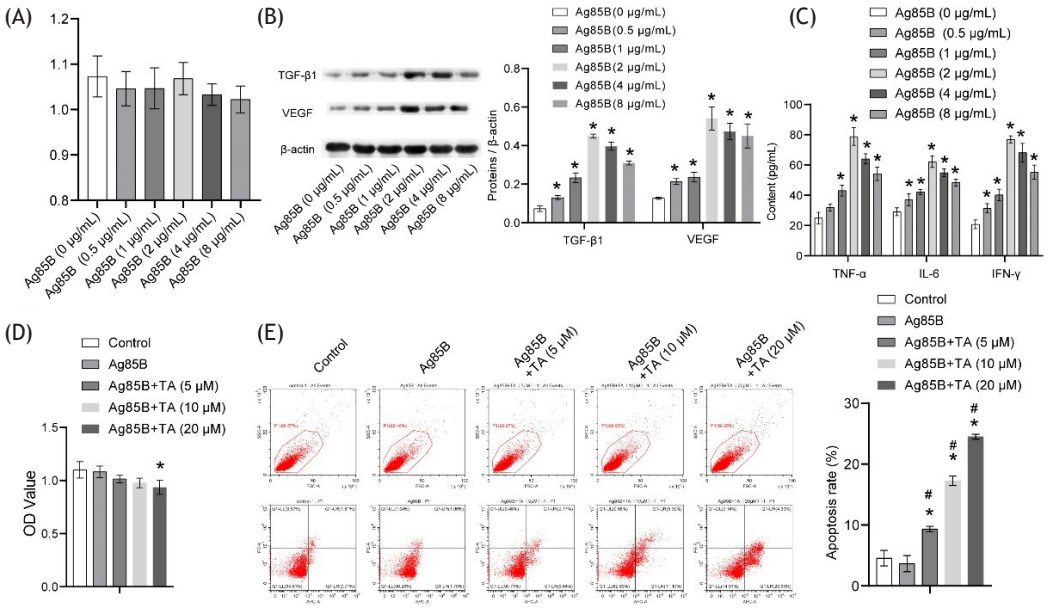

Figure 2 significantly induced apoptosis in Ag85B-treated WI-38 cells. WI-38 cells were treated with 0.5-, 1-, 2-, 4-, or 8-μg/mL Ag85B. (A) The viability of WI-38 cells was tested by CCK-8 assay. (B) The protein levels of VEGF and TGF-β1 in WI-38 cells were investigated by Western blot analysis. (C) The concentrations of IL-6, TNF-α, and IFN-γ in WI-38 cell supernatants were assessed by ELISA. (D) WI-38 cells were treated with Ag85B (2 μg/mL), Ag85B (2 μg/mL), and TA(5 μM), Ag85B and TA (10 μM), or Ag85B (2 μg/mL) and TA (20 μM). The viability of WI-38 cells was tested by CCK-8 assay. (E) The apoptosis rate of WI-38 cells was detected by flow cytometry. *P < 0.05, compared to Ag85B(0 μg/mL). #P < 0.05, compared to Ag85B.

Triamcinolone acetonide reversed Ag85B-induced fibrosis and inhibition of autophagy in WI-38 cells

In order to investigate the function of TA in fibrosis during TSTB, Western blot analysis and ICC were performed. The data revealed that the expressions of VEGF and TGF-β1 in WI-38 cells were notably upregulated by Ag85B, which were significantly rescued by TA (Figures 3A and B). In addition, Ag85B notably upregulated the expression of p62 and inhibited the levels of LC3II/I and Beclin1, while these phenomena were destroyed by TA (Figure 3C). Consistently, the level of LC3 in WI-38 cells was markedly decreased by

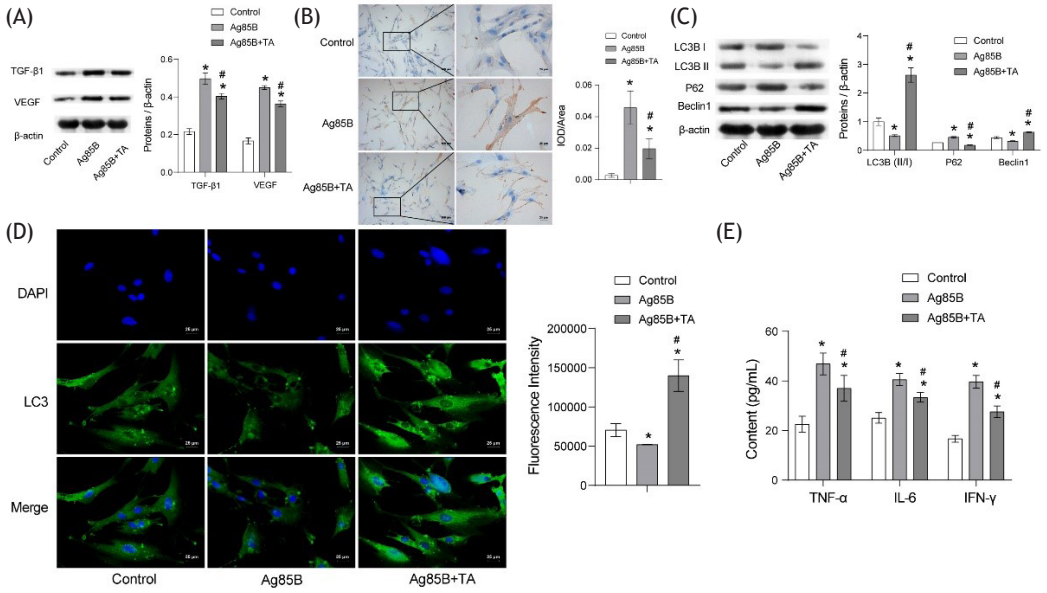

Figure 3 TA reversed Ag85B-induced fibrosis, inflammation, and inhibition of autophagy in WI-38 cells. (A) The protein levels of VEGF and TGF-β1 in WI-38 cells were investigated by Western blot analysis. (B) The level of VEGF in WI-38 cells was investigated by ICC staining. (C) The protein levels of LC3 II/I, Beclin1, and p62 in WI-38 cells were investigated by Western blot analysis. (D) The level of LC3 in WI-38 cells was investigated by immunofluorescence staining. (E) The concentrations of IL-6, TNF-α, and IFN-γ in WI-38 cell supernatants were assessed by ELISA. *P < 0.05, compared to control. #P < 0.05, compared to Ag85B.

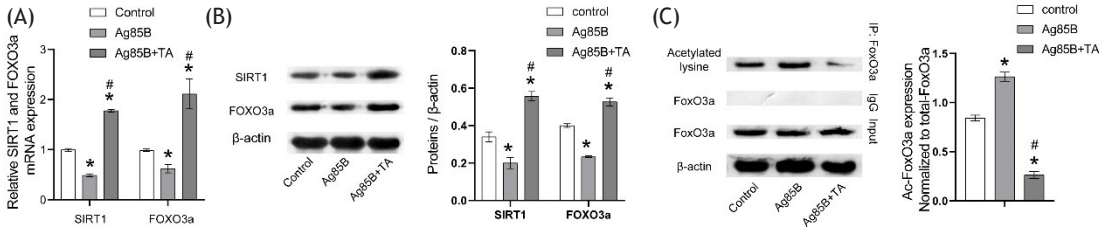

Figure 4 TA restored Ag85B-inhibited SIRT1 and FOXO3a levels in WI-38 cells. (A) The levels of SIRT1 and FOXO3a in WI-38 cells were investigated by RT-qPCR. (B and C) The protein levels of FOXO3a, ac-FOXO3a, and FOXO3a in WI-38 cells were assessed by Western blot analysis. *P < 0.05, compared to control. #P < 0.05, compared to Ag85B.

Ag85B, which was restored by TA (Figure 3D). Furthermore, the concentrations of IL-6, IFN-γ, and TNF-α in WI-38 cell supernatants were significantly upregulated by Ag85B, while the effects of Ag85B on these cytokines were notably suppressed in the presence of TA (Figure 3E). To sum up, TA reversed Ag85B-induced fibrosis, inflammation, and inhibition of autophagy in WI-38 cells.

Triamcinolone acetonide restored Ag85B-inhibited SIRT1 and FOXO3a expressions in WI-38 cells

In order to detect the function of TA in the SIRT1/FOXO3a pathway, RT-qPCR and Western blot analysis were performed. The levels of SIRT1 and FOXO3a in WI-38 cells were markedly inhibited by Ag85B (Figures 4A and B), which were significantly reversed by TA. In contrast, Ag85B-induced activation of ac-FOXO3a was markedly restored in the presence of TA (Figure 4C). In summary, TA restored Ag85B-inhibited SIRT1 and FOXO3a expressions in WI-38 cells.

Knockdown of SIRT1 reversed triamcinolone acetonide-mediated autophagy in Ag85B-treated WI-38 cells

In order to confirm further the relation between TA and SIRT1 in TSTB, RT-qPCR and Western blot analysis were performed. As shown in Figures 5A and B, TA-induced upregulation of SIRT1 and FOXO3a in Ag85B-treated WI-38 cells was notably abolished by SIRT1 siRNA. In addition, the level of ac-p65 in Ag85B-treated WI-38 cells was significantly decreased by TA, while the effect of TA was markedly abolished by SIRT1 silencing (Figure 5B). Next, the effect of TA on LC3II/I, p62, and Beclin1 in Ag85B-treated WI-38 cells was notably alleviated by SIRT1 siRNA (Figures 5C–E). Furthermore, the anti-inflammatory effect of TA on Ag85B-treated WI-38 cells was markedly destroyed by silencing of SIRT1 (Figure 5F). Taken together, the inhibition of SIRT1 reversed TA-mediated autophagy in Ag85B-treated WI-38 cells.

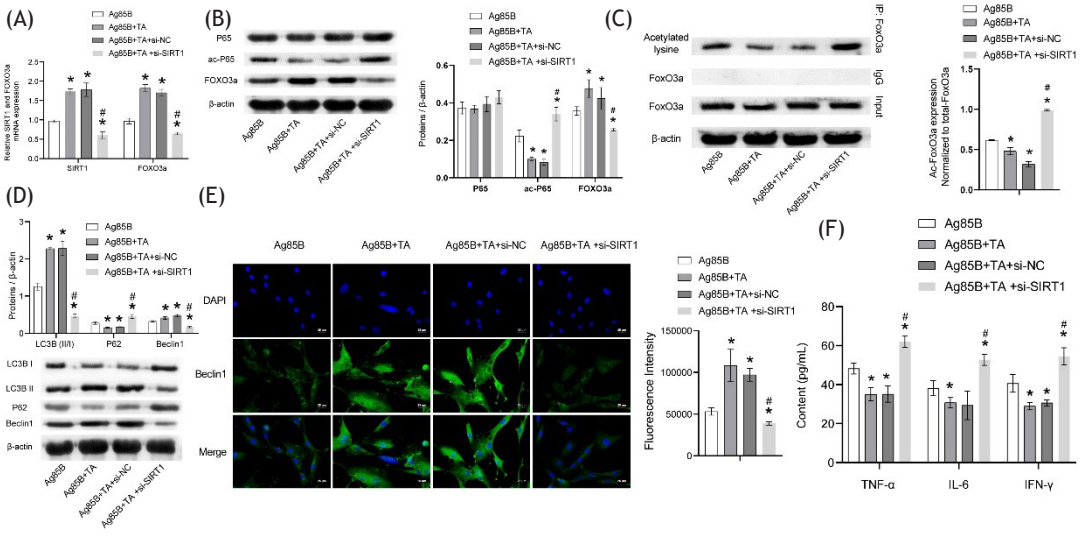

Figure 5 Knockdown of SIRT1 reversed TA-mediated autophagy in Ag85B-treated WI-38 cells. (A) The levels of SIRT1 and FOXO3a in WI-38 cells were investigated by RT-qPCR. (B and C) The protein levels of p65, ac-p65, FOXO3a, and ac-FOXO3a in WI-38 cells were investigated by Western blot analysis. (D)The protein levels of LC3 II/I, p62, and Beclin1 in WI-38 cells were investigated by Western blot analysis. (E) The level of Beclin1 in WI-38 cells was observed by immunofluorescence staining. (F) The concentrations of IL-6, TNF-α, and IFN-γ in WI-38 cell supernatants were assessed by ELISA. *P < 0.05, compared to Ag85B. #P < 0.05, compared to Ag85B+TA+si-NC.

SIRT1 overexpression enhanced the effect of triamcinolone acetonide on TSTB-like model by inducing autophagy

In order to verify further the relation between SIRT1 and autophagy in TA-mediated TSTB progression, the CCK-8 assay was performed. The data revealed that TA slightly inhibited the viability of Ag85B-treated WI-38 cells, and SIRT1 overexpression further enhanced the effect of TA (Figure 6A). However, this phenomenon was rescued in the presence of 3-MA (Figure 6A). In addition, TA significantly induced the apoptosis of Ag85B-treated WI-38 cells, and the apoptotic effect was further increased by pcDNA3.1-SIRT1 (Figure 6B). Nevertheless, the effect of pcDNA3.1-SIRT1 was partially restored in the presence of 3-MA (Figure 6B). Meanwhile, SIRT1 overexpression further enhanced the effect of TA on autophagy-related and fibrotic proteins (LC3, p62, Beclin1, TGF-β1, and VEGF), while 3-MA reversed these phenomena (Figure 6C). Consistently, the anti-inflammatory effect of TA was further enhanced by pcDNA3.1-SIRT1, while this phenomenon was partly rescued in the presence of 3-MA (Figure 6D). In summary, SIRT1 overexpression enhanced the effect of TA on TSTB by inducing autophagy.

Discussion

In mice with skin wound healing, TA inhibited myofibroblast tissue infiltration.[13] TA is widely used in the treatment of fibrosis-related diseases via TGF pathway, such as keloids.[16,17] Consistently, this study found that TA could inhibit fibrosis by the downregulation of TGF-β1 and VEGF. Our research first explored the function of TA in TSTB-like model, suggesting that TA might act as an inhibitor in the progression of TSTB. Generally speaking, the function of TA in TSTB-like model suggested that TSTB progression could be closely related to the activation of autophagy, which provided clinicians new ideas on TSTB treatment.

Mycobacterium TB is the main pathogen of TB and an important cause of TSTB.[3,4] The SARS-CoV-2 spike protein subunit S1 was used to construct a COVID-19-like model.[18] Similarly, Ag85B was utilized to build a TSTB-like model.

TGF-β1 is a key mediator of TGF-β signaling, which is reported to promote fibrosis.[19,20] In addition, VEGF is also involved in the progression of fibrosis as its activation could promote fibrosis.[21,22] Thus, it could be suggested that TA inhibited fibrosis by the inhibition of TGF-β1 and VEGF.

Autophagy could play an important role in cellular processes.[23,24] Despite their distinct mechanisms and functions, autophagy and apoptosis are closely related. More importantly, autophagy is essential for apoptosis, as it often regulates apoptosis.[25] Hence, it could be suggested that TA reversed Ag85B-induced cell apoptosis by regulating autophagy. The p62, LC3, and Beclin1 proteins were crucial players in autophagy.[26,27] The present work has consistently verified that TA reversed Ag85B-induced inhibition of cell autophagy by modulating these proteins.

SIRT1 is a sirtuin (a family of signaling proteins) with anti-inflammatory and anti-fibrotic effects on the liver, kidney, and skin. SIRT1 is protective against systemic sclerosis-associated pulmonary fibrosis by reducing pro-inflammatory and pro-fibrotic processes.[28] SIRT1 plays a vital role in NF-κB-dependent pro-inflammation in the lungs of smokers and chronic obstructive pulmonary disease (COPD) patients.[29] SIRT1 also regulates the inflammatory response of fibroblasts by inactivating the sirtuin activity-dependent

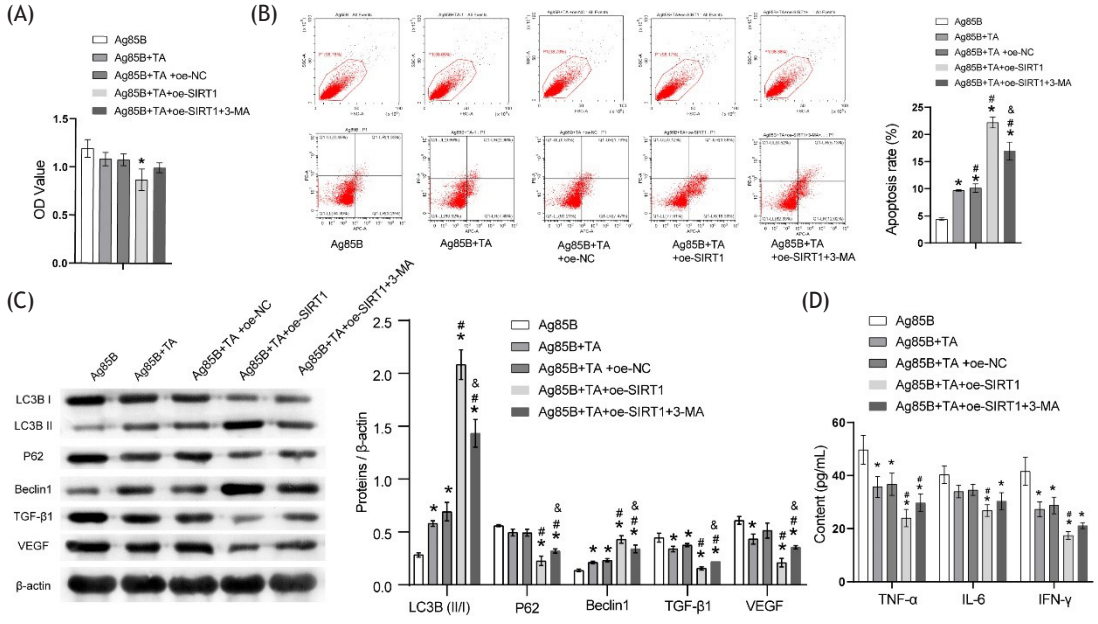

Figure 6 SIRT1 overexpression enhanced the effect of TA on Ag85B-treated WI-38 cells by inducing autophagy. (A) The optical density (OD) of WI-38 cells was tested by CCK-8 assay. (B) The apoptosis of WI-38 cells was assessed by flow cytometry. (C) The protein levels of LC3 II/I, p62, VEGF, TGF-β1, and Beclin1 in WI-38 cells were investigated by Western blot analysis. (D) The concentrations of IL-6, TNF-α, and IFN-γ in WI-38 cell supernatants were assessed by ELISA. *P < 0.05, compared to Ag85B. #P < 0.05, compared to Ag85B + TA + oe-NC. &P < 0.01, compared to Ag85B + TA + oe-SIRT1.

NF-κB pathway.[30] SIRT1 can deacetylate members of the FOXO3 family and affect downstream pathways that control autophagy.[31] Activation of SIRT1/FOXO3a-mediated autophagy can ameliorate hepatic ischemia-reperfusion injury.[32] In addition, SIRT1 and FOXO3 could interact with the subunit of RelA/p65, inhibit NF-κB activity, and participate in inflammatory responses.[33] SIRT1/FOXO3a signaling was involved in the progression of fibrosis and autophagy.[34,35] In our study, the SIRT1/FOXO3a levels were downregulated in TPTA and TSTS tissues, and TA could activate SIRT1/FOXO3a signaling in Ag85B-treated cells. Therefore, it could be concluded that TA could reverse the effect of Ag85B on fibrosis and autophagy by mediating SIRT1/FOXO3a signaling. Meanwhile, SIRT1/FOXO3a can regulate LPS-induced apoptosis in C2C12 myotube cells.[36] Our study found that TA might induce Ag85B-treated cell apoptosis by regulating SIRT1/FOXO3a signaling.

Acetylation and protein levels are usually correlated inversely.[37,38] In this study, we found that TA was able to decrease the acetylation of FOXO3a, increasing the protein levels of SIRT1 and FOXO3a. FOXO3a is a key member of cell growth, and its upregulation could inhibit cell proliferation.[39] Meanwhile, FOXO3a could be negatively regulated by SIRT1.[40,41] Thus, it could be suggested that TA was able to regulate the expression of FOXO3a through SIRT1/FOXO3a acetylation pathway.

This research has some limitations, which are as follows: (1) Animal study is required to verify further the impact of TA in TSTB; (2) the mechanism by which TA regulated SIRT1 remained unclear; (3) the stage of TB infection at which the use of TA would achieve the best therapeutic effect remained unclear. Hence, further exploration in animal and clinical experiments are essentially required in the future.

Conclusion

Triamcinolone acetonide induces the autophagy of fibroblasts in the TSTB-like model by mediating the SIRT1/FOXO3 pathway. This study proposes a new theoretical basis for exploring strategies against TSTB. However, it requires further exploration whether TA can be used as a potential new drug against TSTB.

Acknowledgments

This study was supported by the Clinical Medical Technology Innovation Guidance Project of Hunan Province (2020SK50701), and the Natural Science Foundation of Changsha City (kq2014187).

Author contributions

Li Luo and Zhou Lei contributed to conceptualization, data curation, formal analysis, methodology, and writing of original draft of the study. Linzi Luo, Dan Feng, Yan Ding, Zhibin Lu, and Ganjuan Nie contributed to conceptualization, investigation, methodology, and validation of the study. Liqiong Bai and Yangbao Xiao contributed to acquisition of funding, investigation, supervision, and writing (review and editing) of the paper. All authors read and approved the final manuscript.

Availability of data and materials

The data used to support the findings of this study are available from the corresponding author upon request.

Ethical approval

The study was approved by the Hunan Provincial Chest Hospital Medical Ethics Committee (LS2021011404). The research was conducted according to the World Medical Association Declaration of Helsinki. The researchers explained all the information of the study to the subjects. All the participants provided written informed consent before sampling.

Conflict of interest

The authors stated that there were no conflicts of interest to disclose.

References

1. Pathak V, Shepherd RW, Shojaee S. Tracheobronchial tuberculosis. J Thorac Dis. 2016;8(12):3818–25. https://doi.org/10.21037/jtd.2016.12.75
2. Lee KCH, Tan S, Goh JK, Hsu AAL, Low SY. Long-term outcomes of tracheobronchial stenosis due to tuberculosis (TSTB) in symptomatic patients: Airway intervention vs. conservative management. J Thorac Dis. 2020;12(7):3640–50. https://doi.org/10.21037/JTD-20-670
3. Lee HS, Hua HS, Wang CH, Yu MC, Chen BC, Lin CH. Mycobacterium tuberculosis induces connective tissue growth factor expression through the TLR2-JNK-AP-1 pathway in human lung fibroblasts. FASEB J. 2019;33(11):12554–64. https://doi.org/10.1096/fj.201900487R
4. Kim Y, Kim K, Joe J, Park H, Lee M, Kim Y, et al. Changes in the levels of interferon-gamma and transforming growth factor-beta influence bronchial stenosis during the treatment of endobronchial tuberculosis. Respiration. 2007;74(2):202–7. https://doi.org/10.1159/000097491
5. Gideon HP, Phuah J, Myers AJ, Bryson BD, Rodgers MA, Coleman MT, et al. Variability in tuberculosis granuloma T cell responses exists, but a balance of pro- and anti-inflammatory cytokines is associated with sterilization. PLoS Pathog. 2015;11(1):e1004603. https://doi.org/10.1371/journal.ppat.1004603
6. Karagiannidis C, Velehorschi V, Obertrifter B, Macha HN, Linder A, Freitag L. High-level expression of matrix-associated transforming growth factor-beta1 in benign airway stenosis. Chest. 2006;129(5):1298–304. https://doi.org/10.1378/chest.129.5.1298
7. Kuma A, Komatsu M, Mizushima N. Autophagy-monitoring and autophagy-deficient mice. Autophagy. 2017;13(10):1619–28. https://doi.org/10.1080/15548627.2017.1343770
8. Qin EY, Gan LM, Gan JH, Li Y, Li WT, Hou CC, et al. [Expression and significance of autophagy in rabbit model of tracheal stenosis]. Zhonghua Yi Xue Za Zhi (Chinese). 2017;97(48):3816–20.
9. Khan A, Bakhru P, Saikolappan S, Das K, Soudani E, Singh CR, et al. An autophagy-inducing and TLR-2 activating BCG vaccine

induces a robust protection against tuberculosis in mice. NPJ Vaccines. 2019;4:34. https://doi.org/10.1038/s41541-019-0122-8
10. Oh DS, Lee HK. Autophagy protein ATG5 regulates CD36 expression and anti-tumor MHC class II antigen presentation in dendritic cells. Autophagy. 2019;15(12):2091–106. https://doi.org/10.1080/15548627.2019.1596493
11. Ryter SW, Choi AM. Autophagy in lung disease pathogenesis and therapeutics. Redox Biol. 2015;4:215–25. https://doi.org/10.1016/j.redox.2014.12.010
12. Athanasiadis Y, Tsatsos M, Sharma A, Hossain P. Subconjunctival triamcinolone acetonide in the management of ocular inflammatory disease. J Ocul Pharmacol Ther. 2013;29(6):516–22. https://doi.org/10.1089/jop.2012.0208
13. Nakajima N, Hashimoto S, Sato H, Takahashi K, Nagoya T, Kamimura K, et al. Efficacy of gelatin hydrogels incorporating triamcinolone acetonide for prevention of fibrosis in a mouse model. Regen Ther. 2019;11:41–6. https://doi.org/10.1016/j.reth.2019.04.001
14. Chen AD, Chen RF, Li YT, Huang YT, Lin SD, Lai CS, et al. Triamcinolone acetonide suppresses keloid formation through enhancing apoptosis in a nude mouse model. Ann Plast Surg. 2019;83(4S, Suppl 1):S50–4. https://doi.org/10.1097/SAP.0000000000002090
15. Zhou W, Yu Q, Ma J, Xu C, Wu D, Li C. Triamcinolone acetonide combined with 5-fluorouracil suppresses urethral scar fibroblasts autophagy and fibrosis by increasing miR-192-5p expression. Am J Transl Res. 2021;13(6):5956–68.
16. Hietanen KE, Järvinen TA, Huhtala H, Tolonen TT, Kuokkanen HO, Kaartinen IS. Treatment of keloid scars with intralesional triamcinolone and 5-fluorouracil injections—A randomized controlled trial. J Plast Reconstr Aesthet Surg. 2019;72(1):4–11. https://doi.org/10.1016/j.bjps.2018.05.052
17. Carroll LA, Hanasono MM, Mikulec AA, Kita M, Koch RJ. Triamcinolone stimulates bFGF production and inhibits TGF-beta1 production by human dermal fibroblasts. Dermatol Surg. 2002;28(8):704–9. https://doi.org/10.1097/00042728-200208000-00011 https://doi.org/10.1046/j.1524-4725.2002.02012.x
18. Colunga Biancatelli RML, Solopov PA, Sharlow ER, Lazo JS, Marik PE, Catravas JD. The SARS-CoV-2 spike protein subunit S1 induces COVID-19-like acute lung injury in K18-hACE2 transgenic mice and barrier dysfunction in human endothelial cells. Am J Physiol Lung Cell Mol Physiol. 2021;321(2):L477–84. https://doi.org/10.1152/ajplung.00223.2021
19. Meng XM, Nikolic-Paterson DJ, Lan HY. TGF-beta: The master regulator of fibrosis. Nat Rev Nephrol. 2016;12(6):325–38. https://doi.org/10.1038/nrneph.2016.48
20. Xu F, Liu C, Zhou D, Zhang L. TGF-beta/SMAD pathway and its regulation in hepatic fibrosis. J Histochem Cytochem. 2016;64(3):157–67. https://doi.org/10.1369/0022155415627681
21. Sun J, Shi L, Xiao T, Xue J, Li J, Wang P, et al. microRNA-21, via the HIF-1alpha/VEGF signaling pathway, is involved in arsenite-induced hepatic fibrosis through aberrant cross-talk of hepatocytes and hepatic stellate cells. Chemosphere. 2021;266:129177. https://doi.org/10.1016/j.chemosphere.2020.129177
22. Kariya T, Nishimura H, Mizuno M, Suzuki Y, Matsukawa Y, Sakata F, et al. TGF-beta1-VEGF-A pathway induces neoangiogenesis with peritoneal fibrosis in patients undergoing peritoneal dialysis. Am J Physiol Renal Physiol. 2018;314(2):F167–80. https://doi.org/10.1152/ajprenal.00052.2017
23. Li YJ, Lei YH, Yao N, Wang CR, Hu N, Ye WC, et al. Autophagy and multidrug resistance in cancer. Chin J Cancer. 2017;36(1):52. https://doi.org/10.1186/s40880-017-0219-2
24. Kim KH, Lee MS. Autophagy—A key player in cellular and body metabolism. Nat Rev Endocrinol. 2014;10(6):322–37. https://doi.org/10.1038/nrendo.2014.35
25. Parzych KR, Klionsky DJ. An overview of autophagy: Morphology, mechanism, and regulation. Antioxid Redox Signal. 2014;20(3):460–73. https://doi.org/10.1089/ars.2013.5371
26. Mizushima N, Levine B. Autophagy in human diseases. N Engl J Med. 2020;383(16):1564–76. https://doi.org/10.1056/NEJMra2022774
27. Levine B, Kroemer G. Biological functions of autophagy genes: A disease perspective. Cell. 2019;176(1–2):11–42. https://doi.org/10.1016/j.cell.2018.09.048
28. Chu H, Jiang S, Liu Q, Ma Y, Zhu X, Liang M, et al. Sirtuin1 protects against systemic sclerosis-related pulmonary fibrosis by decreasing proinflammatory and profibrotic processes. Am J Respir Cell Mol Biol. 2018;58(1):28–39. https://doi.org/10.1165/rcmb.2016-0192OC
29. Rajendrasozhan S, Yang SR, Kinnula VL, Rahman I. SIRT1, an antiinflammatory and antiaging protein, is decreased in lungs of patients with chronic obstructive pulmonary disease. Am J Respir Crit Care Med. 2008;177(8):861–70. https://doi.org/10.1164/rccm.200708-1269OC
30. Zhu X, Liu Q, Wang M, Liang M, Yang X, Xu X, et al. Activation of Sirt1 by resveratrol inhibits TNF-alpha-induced inflammation in fibroblasts. PLoS One. 2011;6(11):e27081. https://doi.org/10.1371/journal.pone.0027081
31. Tang BL. Sirt1 and the mitochondria. Mol Cells. 2016;39(2):87–95. https://doi.org/10.14348/molcells.2016.2318
32. Lin Y, Sheng M, Weng Y, Xu R, Lu N, Du H, et al. Berberine protects against ischemia/reperfusion injury after orthotopic liver transplantation via activating Sirt1/FOXO3 alpha-induced autophagy. Biochem Biophys Res Commun. 2017;483(2):885–91. https://doi.org/10.1016/j.bbrc.2017.01.028
33. Hwang JW, Rajendrasozhan S, Yao H, Chung S, Sundar IK, Huyck HL, et al. FOXO3 deficiency leads to increased susceptibility to cigarette smoke-induced inflammation, airspace enlargement, and chronic obstructive pulmonary disease. J Immunol. 2011;187(2):987–98. https://doi.org/10.4049/jimmunol.1001861
34. Zheng LN, Guo FQ, Li ZS, Wang Z, Ma JH, Wang T, et al. Dexmedetomidine protects against lidocaine-induced neurotoxicity through SIRT1 downregulation-mediated activation of FOXO3a. Hum Exp Toxicol. 2020;39(9):1213–23. https://doi.org/10.1177/0960327120914971
35. Li H, Chou P, Du F, Sun L, Liu J, Wang W. Depleting microRNA-183-3p improves renal tubulointerstitial fibrosis after acute kidney injury via SIRT1/PUMA/FOXO3a deacetylation. Life Sci. 2021;269:119017. https://doi.org/10.1016/j.lfs.2021.119017
36. Zhao Y, Jiang Q, Zhang X, Zhu X, Dong X, Shen L, et al. l-arginine alleviates LPS-induced oxidative stress and apoptosis via activating SIRT1-AKT-Nrf2 and SIRT1-FOXO3a signaling pathways in C2C12 myotube cells. Antioxidants (Basel). 2021;10(12):1957. https://doi.org/10.3390/antiox10121957
37. Diallo I, Seve M, Cunin V, Minassian F, Poisson JF, Michelland S, et al. Current trends in protein acetylation analysis. Expert Rev Proteomics. 2019;16(2):139–59. https://doi.org/10.1080/14789450.2019.1559061
38. Baeza J, Smallegan MJ, Denu JM. Mechanisms and dynamics of protein acetylation in mitochondria. Trends Biochem Sci. 2016;41(3):231–44. https://doi.org/10.1016/j.tibs.2015.12.006
39. Chen H, Hu X, Yang R, Wu G, Tan Q, Goltzman D, et al. SIRT1/FOXO3a axis plays an important role in the prevention of mandibular bone loss induced by 1,25(OH)2D deficiency. Int J Biol Sci. 2020;16(14):2712–26. https://doi.org/10.7150/ijbs.48169
40. Zou Z, Liu B, Zeng L, Yang X, Huang R, Wu C, et al. Cx43 inhibition attenuates sepsis-induced intestinal Injury via downregulating ROS transfer and the activation of the JNK1/Sirt1/FOXO3a signaling pathway. Mediators Inflamm. 2019;2019:7854389. https://doi.org/10.1155/2019/7854389
41. Karbasforooshan H, Karimi G. The role of SIRT1 in diabetic cardiomyopathy. Biomed Pharmacother. 2017;90:386–92. https://doi.org/10.1016/j.biopha.2017.03.056